DiPyMe in SDS Micelles – Artefacts and their Implications on the Interpretation of Micellar Properties

Michael Fowler, Victoria Hisko, Jason Henderson, Remi Casier, Lu Li, Janine Lydia Thoma,

Jean Duhamel*

Institute for Polymer Research, Waterloo Institute for Nanotechnology, Department of

Chemistry, University of Waterloo, 200 University Avenue, Waterloo, On N2L 3G1, Canada

* To Whom correspondence should be addressed.

ABSTRACT

This study provides experimental evidence that di(1-pyrenylmethyl) ether or DiPyMe, a well-known fluorescent probe employed to determine the microviscosity of surfactant or polymeric micelles, is being hydrolyzed in the presence of water upon UV irradiation. This effect was established from the careful analysis of the fluorescence spectra and decays acquired with aqueous solutions of DiPyMe dissolved in micelles of sodium dodecyl sulfate (SDS). The size of the SDS micelles could be adjusted from an aggregation number (N_{agg}) of 70 to 172 by increasing the ionic strength of the aqueous solution from 0.0 to 0.5 M NaCl. Hydrolysis of DiPyMe was much reduced in the larger SDS micelles. While degradation of DiPyMe in aqueous solutions of SDS micelles affected the analysis of the fluorescence spectra, Model Free Analysis (MFA) of the fluorescence decays of DiPyMe could reliably retrieve the rate constant $<k>$ of excimer formation for DiPyMe. After calibration with mixtures of organic solvents of known macroscopic viscosity, the $<k>$ values obtained for DiPyMe yielded the microviscosity ($\mu\eta$) of the SDS micelles as a function of salt concentration. $\mu\eta$ was found to increase from 4.0 to 8.8 mPa.s as the salt concentration increased from 0.0 to 0.5 M. This study demonstrated that, regardless of the problem of its hydrolysis that jeopardizes its use in steady-state fluorescence experiments, DiPyMe remains an extremely valuable probe to describe the microviscosity of hydrophobic domains in aqueous solution, as long as its decays are analyzed with a model that accounts for the presence of degradation products as the MFA does.

INTRODUCTION

Di(1-pyrenylmethyl) ether also referred to as DiPyMe[1] belongs to the large family of bipyrenyl compounds that are composed of two pyrene moieties separated by a linear chain and which have been studied in great detail over the last four decades.[1-10] The photophysical properties of dipyrenyl alkanes first introduced in 1976 by Zachariasse[2] have been carefully characterized in the 1980s and 1990s, particularly the effect that the spacer length between the two pyrene groups had on their ability to form an excimer.[2-5,8,9] The salient features of these studies were that, for linkers long enough to avoid specific unfavorable conformations that in some cases prevented excimer formation all together, the efficiency of pyrene excimer formation decreased with increasing linker length and that up to two types of excimer species could be detected. Among bipyrenyl molecules, DiPyMe with a dimethyl ether linkage[1,11-20] and di(1-pyrenyl)propane (DiPyPr) with a propylene linker[11,21-30] have been the most studied probably because their short three atom-long spacer endowed them with the smallest molecular dimension of all bipyrenyl compounds and excimer formation between an excited and ground-state pyrene took place diffusionally and very efficiently due to the short linker holding the pyrene groups in close vicinity. Consequently, DiPyMe and DiPyPr were small enough to fit inside any hydrophobic microdomain generated by molecular or polymeric surfactants in aqueous solution while the diffusion-controlled process of pyrene excimer formation provided information about the local viscosity also referred to as microviscosity of the medium DiPyMe and DiPyPr were embedded in.

The synthesis of DiPyMe was first published in 1980 and its photophysical properties, particularly the dependency of pyrene excimer formation on the microviscosity of the environment, were applied to probe the phase transitions in lipid membranes that affected their fluidity as a function of temperature.[1,11] These studies monitored the ratio of excimer-to-monomer

intensity, namely the I_E/I_M ratio, as a function of temperature and searched for a discontinuity in the I_E/I_M-vs-T profiles as an indication of a transition in membrane fluidity. Besides its ability to form excimer efficiently, DiPyMe is also endowed with other advantageous features rendering it an attractive fluorophore to probe micellar systems in aqueous solutions. First the fluorescence spectrum of DiPyMe responds to the polarity of its local environment from the I_1/I_3 ratio where I_1 and I_3 represent the fluorescence intensities of the first and third peak in the fluorescence spectrum of the pyrene monomer, respectively.[11] This was a surprising outcome because the well-known sensitivity of pyrene to the polarity of its environment is the result of its symmetry-forbidden 0-0 transition[31-33] which is no longer forbidden upon derivatization of pyrene[34] as in DiPyPr.[11] Somehow, the oxygen in the β-position of the pyrene groups of DiPyMe seems to re-symmetrize the electronic wavefunction of pyrene which restores the sensitivity of the pyrene moieties of DiPyMe to the polarity of its local environment.[11-13] Second DiPyMe can be transferred from the water phase to hydrophobic microdomains without repeated freeze-drying cycles of the aqueous solution which are otherwise necessary to bring DiPyPr into the hydrophobic interior of surfactant micelles.[23,26] This different behaviour is certainly a consequence of the more polar ether linker of DiPyMe that increases its solubility in water compared to DiPyPr and facilitates its transport through the water phase into the micelles. Finally the low oxygen concentration found in water makes the outgassing of oxygen by bubbling nitrogen, a mandatory step for pyrene dissolved in organic solvents, unnecessary for pyrene dissolved in an aqueous solution of surfactant micelles. In practice, this represents a welcome simplification since the large amount of foam generated by bubbling nitrogen in aqueous solutions of a surfactant is an experimental complication.

Based on all these interesting features, it is thus hardly surprising that DiPyMe has been employed to probe a wide range of heterogeneous media in aqueous solutions. In particular, lipid

membranes,[1,11,14] polymeric micelles,[12,13,15,16,18,20] and polymer matrices[19] have all been investigated with DiPyMe. Considering such a sustained interest over a time period spanning more than three decades, it is thus somewhat surprising that the hydrolysis of DiPyMe in aqueous solutions has never been reported. This study demonstrates that irradiation of DiPyMe in aerated aqueous solutions of SDS micelles results in the hydrolysis of DiPyMe and the formation of 1-pyrenemethanol which affects strongly the fluorescence spectrum of DiPyMe, and thus the ratio I_E/I_M which is normally used to estimate the microviscosity of the medium where DiPyMe is dissolved.

In these experiments, the fluorescence spectra and decays of DiPyMe were monitored in aqueous solutions of 50 mM SDS which were prepared with NaCl concentrations ranging from 0.0 to 0.5 M. These conditions ensured the presence of a large excess of SDS micelles that could solvate individual DiPyMe molecules in separate SDS micelles. The SDS micelles were carefully characterized by using molecular pyrene and its ability to form an excimer to determine their aggregation numbers (N_{agg}) and rate constant of excimer formation (k_q) between one excited pyrene and one ground-state pyrene located in a same micelle. Irradiation of the DiPyMe solutions by the steady-state fluorometer over a set irradiation time led to hydrolysis of DiPyMe which could be easily detected from the significant increase in the monomer fluorescence intensity and the associated drop in the I_E/I_M ratio. Global analysis of the monomer and excimer fluorescence decays with the Model Free Analysis (MFA)[35-37] yielded parameters that provided a complete description of the behaviour of the different pyrene species present in solution. This study led to the conclusion that while the hydrolysis of DiPyMe upon irradiation compromised the determination of the microviscosity of the hydrophobic domains in aqueous solution based on the traditional analysis of the I_E/I_M ratio, the microviscosity ($\mu\eta$) of the hydrophobic interior of SDS

micelles could still be determined quantitatively by comparing the average rate constant of excimer formation <*k*> obtained for DiPyMe in aqueous SDS solutions with the <*k*> values obtained as a function of solution viscosity for mixtures of organic solvents. These experiments led to the finding that the microviscosity of SDS micelles increased from 4.0 mPa.s without salt up to 8.8 mPa.s with 0.3 M salt without changing much within experimental error for salt concentrations greater than 0.3 M. The effect of $\mu\eta$ and N_{agg} on k_q found for pyrene excimer formation were investigated and led to the conclusion that SDS micelles transition from a spherical to a cylindrical morphology at a salt concentration of 0.3 M.

While the results presented in this study provide a first complete characterization of SDS micelles in terms of size (N_{agg}) and microviscosity based solely on the fluorescence of different pyrene derivatives, certainly the most important aspect of this study was not the observation that DiPyMe hydrolyzes in aqueous solution of SDS but rather the demonstration that MFA of the pyrene monomer and excimer decays of a molecule that can form excimer between two pyrene labels provides a quantitative description in terms of molar fractions and rate constant of excimer formation of all the pyrene species present in the solution. This study is thus an additional illustration of the as yet unmatched analytical capabilities offered by the MFA to deal with experiments involving complex kinetics of pyrene excimer formation.

EXPERIMENTAL

Materials: Pyrene (Aldrich) was crystallized three times from spectrograde methanol. DiPyMe was prepared from reaction of 1-pyrenemethoxide with 1-pyrenemethylene chloride according to a published procedure.[1,18] 1-Pyrenemethanol used to prepare DiPyMe was purchased from Aldrich. DMSO (reagent), PEG(0.4K), and benzyl alcohol (puriss.) were also purchased from Aldrich.

Distilled in glass tetrahydrofuran (THF) and toluene were obtained from Caledon. Milli-Q water with a resistivity of over 18 MΩ·cm was used to prepare all aqueous solutions.

Preparation of aqueous solutions of SDS and DiPyMe for fluorescence measurements: Samples were prepared by dissolving DiPyMe in THF, measuring its absorbance, and then transferring a sufficient quantity to a vial such that, after evaporation of THF and subsequent addition of 5 mL of aqueous solution of SDS, the absorbance at 345.5 nm would equal 0.2 in a same volume of THF equivalent to a DiPyMe concentration of 2.4×10^{-6} M. Spectra of the molar absorbance coefficient of DiPyMe in THF and 50 mM SDS aqueous solution without salt can be found in Figure S1 in Supporting Information (SI). This low concentration of DiPyMe ensured that the probability of having more than two DiPyMe molecules per SDS micelle was negligible ($Pr(i>1) < 2\times10^{-5}$). An aliquot of a concentrated (100 mM) SDS solution was added to the vial to obtain a final SDS concentration of 50 mM. Similarly, an aliquot of a 5.0 M aqueous solution of NaCl was added such that the salt concentration would vary from 0 to 0.5 M in 0.1 M increments. The final volume of the SDS solution was adjusted with Milli-Q water. The flasks containing the solutions were either placed in a shaker, or had a small stir bar added and were then placed on a stir plate. The flasks were subjected to shaking or stirring for a period of one week.

Fluorescence experiments with DiPyMe in SDS aqueous solutions: Acquisition of the time-resolved fluorescence decays and steady-state fluorescence spectra was conducted according to the following protocol whereby the irradiation time of the samples in the steady-state fluorometer was carefully monitored. First, the time-resolved fluorescence decays of the pyrene monomer and excimer for DiPyMe were acquired since the light source of the time-resolved fluorometer was of sufficiently low power that it did not noticeably degrade DiPyMe. Then the sample was placed in the steady-state fluorometer and the steady-state fluorescence spectrum was acquired. The

samples were left in the steady-state fluorometer until a total of two minutes had elapsed, corresponding to a two-minute irradiation. This process of acquiring the time-resolved fluorescence decays, acquiring the steady-state fluorescence spectrum, and irradiating for a two minutes period in the steady-state fluorometer was then repeated in the same order. After each period of irradiation in the steady-state fluorometer, the sample was mixed by inverting the cell at least five times. To this end, approximately a half-centimetre head space was left in the 1 cm×1 cm fluorescence cell during sample preparation to allow for effective mixing.

Steady-state fluorescence: The fluorescence spectra were acquired using a continuous Xe lamp for excitation that was fitted on a Photon Technology International LS-100 steady-state fluorometer. The aqueous solutions of pyrene and DiPyMe in 50 mM SDS aqueous solutions were excited at a wavelength of 334 and 344 nm, respectively, with the steady-state emission being monitored from 350 to 600 nm. The slits of the excitation and emission monochromators were set to equal 2.0 and 1.0 nm, respectively. The integration time per data point equalled 0.1 s/nm, which ensured that the total irradiation time for acquisition of the entire fluorescence spectrum was less than 30 seconds. Fortunately in the case of the DiPyMe solutions, it was the monomer portion of the spectrum which varied most significantly with irradiation time, and this segment of the spectrum was recorded first and in less than 10 seconds. For both the pyrene and DiPyMe solutions, the monomer and excimer fluorescence intensities were determined by integrating the spectrum from 372 to 378 nm and from 500 to 530 nm, respectively. The I_1/I_3 ratio was determined from the ratio of the I_1 peak at 375 nm and the I_3 peak at 386 nm.

Time-resolved fluorescence: The fluorescence decays for the monomer were acquired with an IBH time-resolved fluorometer with an emission wavelength of 375 nm and 510 nm for the pyrene monomer and excimer, respectively. A NanoLED 340 diode (FWHM = 1.06 ns) was used to excite

the samples. The fluorescence decays of the pyrene monomer in 50 mM SDS solutions with pyrene concentrations ranging from 0.07 to 0.40 mM were fitted with Equation 1.

$$[Py]_{(t)} = [Py]_{(t=0)} \times \exp[-t/\tau_M - < n > (1 - \exp(-k_q t)] \quad (1)$$

In Equation 1, $[Py]_{(t)}$ is the concentration of pyrene at a given time t after the excitation pulse hit the solution at $t = 0$. The lifetime of the monomer of molecular pyrene in SDS micelles (τ_M) was set to equal 175 ns and was fixed in the analysis, <n> was the average number of pyrenes per micelle, and k_q was the rate constant for excimer formation in a micelle that contained one excited and one ground-state pyrene. Since <n> equals [*Py*]/[*Mic*] where [*Mic*] is the concentration of SDS micelles, <n> was found to increase linearly with [*Py*] and the slope of this straight line yielded N_{agg}, the aggregation number of an SDS micelle, as shown in Equation 2. CMC in Equation 2 represents the critical micelle concentration of SDS.

$$< n > = \frac{[Py]}{[Mic]} = N_{agg} \times \frac{[Py]}{[SDS] - CMC} \quad (2)$$

The time-resolved fluorescence decays of DiPyMe in SDS micelles were fitted according to the Model-Free Analysis (MFA) using a fixed τ_M value of 157 ns, corresponding to the lifetime of 1-pyrenemethanol in SDS micelles. The specific program used to fit the fluorescence decays of DiPyMe in SDS aqueous solutions was sumegs36dbg which was developed for this application. This program has one coupled lifetime, one fixed lifetime for τ_M, one fixed decay time for quenched but uncoupled monomers, one floating decay time for pyrene degradation products of

the DiPyMe hydrolysis, and two excimers with lifetimes τ_E and τ_D, both excimers being formed by diffusion or direct excitation of ground-state dimers. The average rate constant of pyrene excimer formation for DiPyMe, $<k>$, and the molar fractions of the different pyrene species in solution were all calculated using equations which have been derived earlier and that are presented in Supporting Information (SI).[35,36,37] MFA of the fluorescence decays of DiPyMe in organic media such as the mixtures of toluene and benzyl alcohol or DMSO and PEG(0.4K) used two coupled decay times and one fixed lifetime (τ_M) to fit the monomer decays and the same coupled decay times plus two lifetimes τ_E and τ_D for the two excimer species. The program used for these fits of the DiPyMe decays in organic solvents was sumegs35bg which can be accessed from the internet (http://fluodecay.uwaterloo.ca/). Except for the mixtures of toluene and benzyl alcohol which were degassed with a gentle flow of nitrogen, all other solutions were left aerated.

RESULTS

The hydrolysis of DiPyMe was monitored in aqueous solutions of SDS with NaCl concentrations ranging from 0.0 to 0.5 M. The presence of salt in an aqueous solution of SDS is known to increase substantially the size of SDS micelles[38,39] and thus should provide larger hydrophobic microdomains in water better able of hosting DiPyMe. Consequently, the critical micelle concentration (CMC) and the aggregation number (N_{agg}) of the SDS micelles were determined as a function of NaCl concentration.

To determine the CMC of SDS in aqueous solution with NaCl concentrations ranging between 0.0 and 0.5 M, the fluorescence of a 7.0×10^{-7} M pyrene aqueous solution was monitored as a function of SDS concentration. As shown in Figures S2 and S3, both the monomer and excimer fluorescence showed strong variations as a function of SDS concentration for a salt

concentration of 0.1 M. The I_1/I_3 ratio decreased precipitously in Figure S4 when the SDS concentration passed through the CMC as the environment of pyrene switched from polar water (I_1/I_3 =1.73; reported value of 1.59[31] and 1.87[32]) to the hydrophobic interior of the SDS micelles (I_1/I_3 = 1.01; reported value of 1.04[31]). The formation of SDS micelles at surfactant concentrations just above the CMC also led to the concentration of pyrene molecules inside the few micelles present in solution which led to excimer formation. As a larger number of SDS micelles formed upon increasing the SDS concentration, the pyrene molecules distributed themselves into different SDS micelles which led to their isolation and a decrease in excimer formation. The SDS concentration obtained at the I_E/I_M peak was selected as the CMC and it was plotted as a function of NaCl concentration in Figure 1A. As the salt concentration increased, the CMC decreased and the CMC values that were obtained agreed very well with those reported in the literature.[38,40]

N_{agg} was determined by preparing 50 mM SDS aqueous solutions with pyrene concentrations ranging between 0.07 and 0.40 mM. For each solution, the fluorescence decays of the pyrene monomer were fitted with Equation 1 that yielded k_q and $<n>$. A plot of $<n>$ versus pyrene concentration yielded straight lines in Figure 1B whose slopes were used to determine N_{agg} based on Equation 2. The N_{agg} values were plotted in Figure 1C. In Figure 1C, N_{agg} increased continuously from 70 to 172 when the NaCl concentration was increased from 0.0 to 0.5 M. The increase in micellar size as a function of salt concentration has been well documented and is due to a transition from spherical to rod-like micelles.[38,41] Its characterization has been the object of numerous reports and is beyond the scope of the present study. What matters at this stage is that a good overall agreement was obtained between our N_{agg} values and those obtained in other studies.

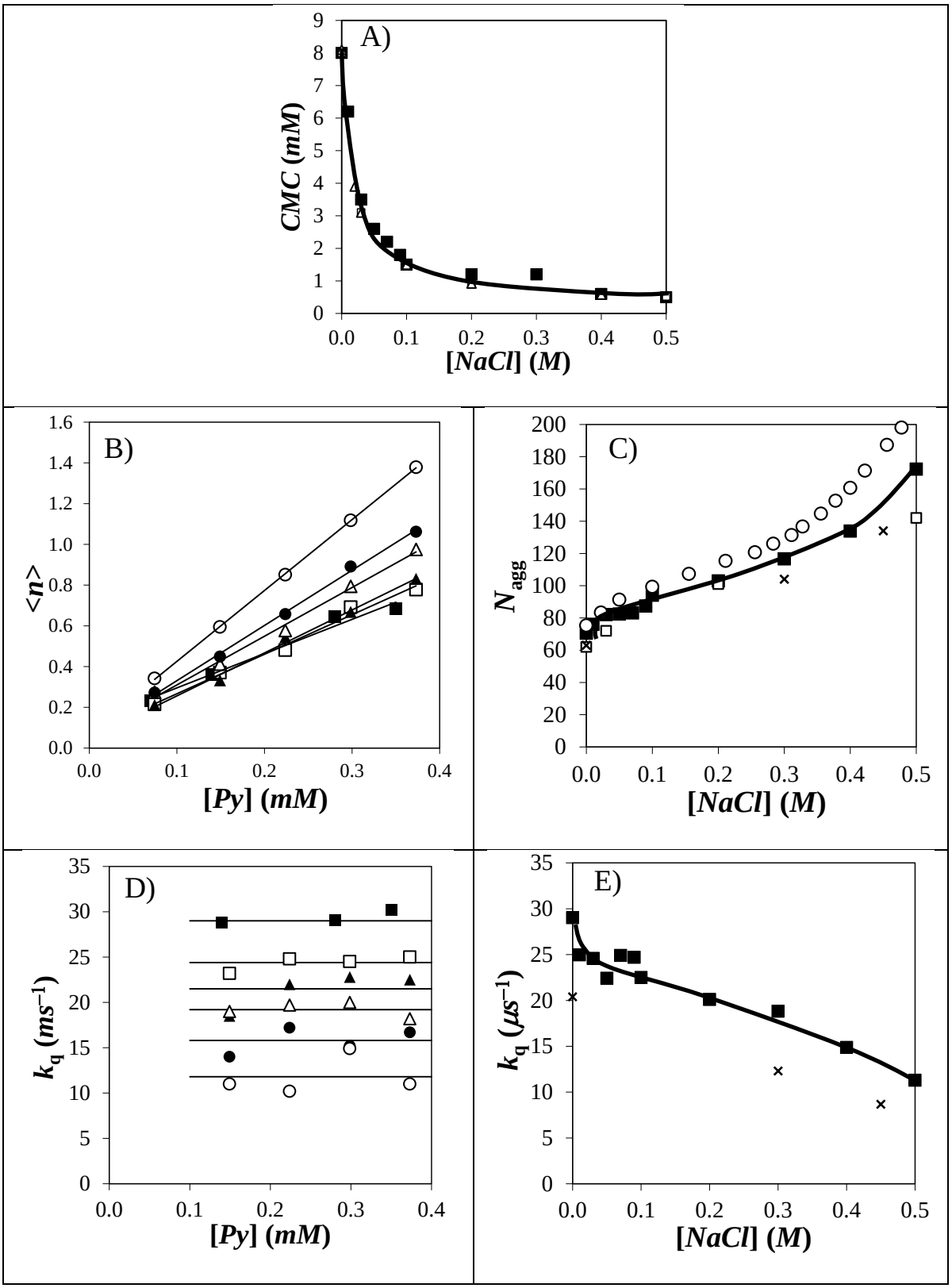

Figure 1. Plot of A) CMC versus [NaCl], B) <*n*> versus [Py], C) N_{agg} versus [NaCl], D) k_q versus [Py], and E) k_q versus [NaCl]. [SDS] = 50 mM. Symbols for figures: A), C), and E): Data obtained

from (■) this work and reference # (□) 38, (○) 39, (△) 40, and (×) 41. B) and D): [NaCl] = (■) 0.0 M, (□) 0.1 M, (▲) 0.2 M, (△) 0.3 M, (●) 0.4 M, and (○) 0.5 M.

Within experimental error, k_q in Figure 1D remained constant as a function of pyrene concentration for a given salt concentration. Its value was averaged and plotted as a function of salt concentration in Figure 1E. k_q is a pseudo-unimolecular rate constant for pyrene excimer formation between one excited pyrene and one ground-state pyrene located in a same SDS micelle whose expression is given in Equation 3.

$$k_q = k_{diff} \times [Py]_{loc} = k_{diff} \times \frac{1}{V_{mic}} \qquad (3)$$

In Equation 3, k_{diff} is the bimolecular rate constant for diffusive encounters between two pyrenes and $[Py]_{loc}$ is the concentration equivalent to one ground-state pyrene inside a micelle ($[Py]_{loc} = 1/V_{mic}$ where V_{mic} is the micellar volume). Equation 3 predicts that, since k_{diff} is inversely proportional to the microviscosity of the micellar interior, k_q is inversely proportional to the microviscosity and N_{agg} since $V_{mic} = N_{agg} \times V_{SDS}$. It is thus reassuring that k_q decreases with increasing salt concentration in Figure 1E since it is inversely proportional to V_{mic} which increases with salt concentration (see N_{agg} in Figure 1C). k_q obtained for pyrene excimer formation is somewhat larger than the k_q value obtained for the quenching of tris(bipyridine) ruthenium chloride ($Ru(bpy)_3$) by 9-methylanthracene (9-MA).[39] The larger k_q size obtained with pyrene comes from the fact that $Ru(bpy)_3$ with its much larger volume and its strong electrostatic binding to the sulfate ions at the micellar surface is much less mobile than pyrene. Thus k_{diff} is smaller in Equation 3 and

the resulting k_q value is also smaller but the general trend of decreasing k_q with increasing salt concentration is also obeyed for $Ru(bpy)_3$ quenched by 9-MA. At this stage, the CMC, N_{agg}, and k_q values of the SDS micelles have been characterized as a function of salt concentration and the results that were obtained are in good agreement with those reported in the literature.[39-40]

DiPyMe was then dissolved in the 50 mM SDS solutions with different salt concentrations and the fluorescence data were obtained according to the strict protocol depicted in the Experimental section. In particular, the fluorescence spectrum of DiPyMe was acquired as a function of irradiation time. As shown in Figure 2A for a DiPyMe aqueous solution with 50 mM SDS without salt, the fluorescence spectrum of DiPyMe underwent massive changes upon irradiation with the I_E/I_M ratio of DiPyMe decreasing from 6.5 to 3.6 over a 10 minute irradiation in the steady-state fluorometer. The origin of this change in the fluorescence spectra was easily identified from the pyrene monomer and excimer fluorescence decays shown in, respectively, Figures 2B and 2C and which were acquired before each 2 min irradiation period in the steady-state fluorometer. While the early part of the monomer decay did not change much, irradiation of the 50 mM SDS solutions with 2.4×10^{-6} M DiPyMe generated a long-lived species whose contribution to the monomer decay increased continuously with increasing irradiation time. Since excimer is formed rapidly due to the proximity of the two pyrenyl moieties in DiPyMe, the short component of the monomer decay was attributed to pyrene excimer formation while the long-lived species must have been a pyrenyl species that was generated upon irradiation of the DiPyMe solution. One obvious origin for this long-lived pyrenyl species would be the hydrolysis of DiPyMe in aqueous solution that would generate two 1-pyrenemethanol (PyMeOH) moieties. Another possibility would be the degradation of one pyrene moiety into a product unable to fluoresce and form an excimer with the other pyrene group. Interestingly those DiPyMe molecules

that did not decompose formed excimer in the same manner as illustrated in Figure 2C where all excimer decays overlapped perfectly regardless of irradiation time. The fluorescence data presented in Figure 2 are actually identical to what would happen to the fluorescence spectrum and monomer and excimer fluorescence decays of a dilute solution of a pyrene labeled macromolecule to which a known amount of free pyrene label was added.[42] The picture that emerges from the fluorescence data shown in Figure 2 is thus consistent with the following description. Upon increased irradiation, more DiPyMe undergoes hydrolysis or decomposes, more PyMeOH is being generated, and the increased contribution of PyMeOH to the fluorescence of DiPyMe leads to an increase in the monomer fluorescence in the fluorescence spectra (Figure 2A), an increase in the contribution of the long-lived species in the fluorescence decays of the pyrene monomer (Figure 2B), and no change in the fluorescence decays of the excimer which is generated by the intact DiPyMe molecules (Figure 2C).

The steady-state fluorescence spectra of the DiPyMe solution acquired as a function of irradiation time and with different salt concentrations were first analyzed to determine the I_E/I_M ratio as a function of salt concentration and irradiation time. The measured values of I_E/I_M are shown in Figure 3A as a function of irradiation time for each salt concentration. For all samples, I_E/I_M decreased with increasing irradiation time, confirming the degradation of DiPyMe. The I_E/I_M ratio varied as a function of salt concentration due to changes in the I_1/I_3 ratio. As described later, an increase in salt led to a larger, more hydrophobic micelle resulting in a smaller I_1 value used to determine I_M in the I_E/I_M ratio. Consequently a lower I_E/I_M ratio was obtained without salt.

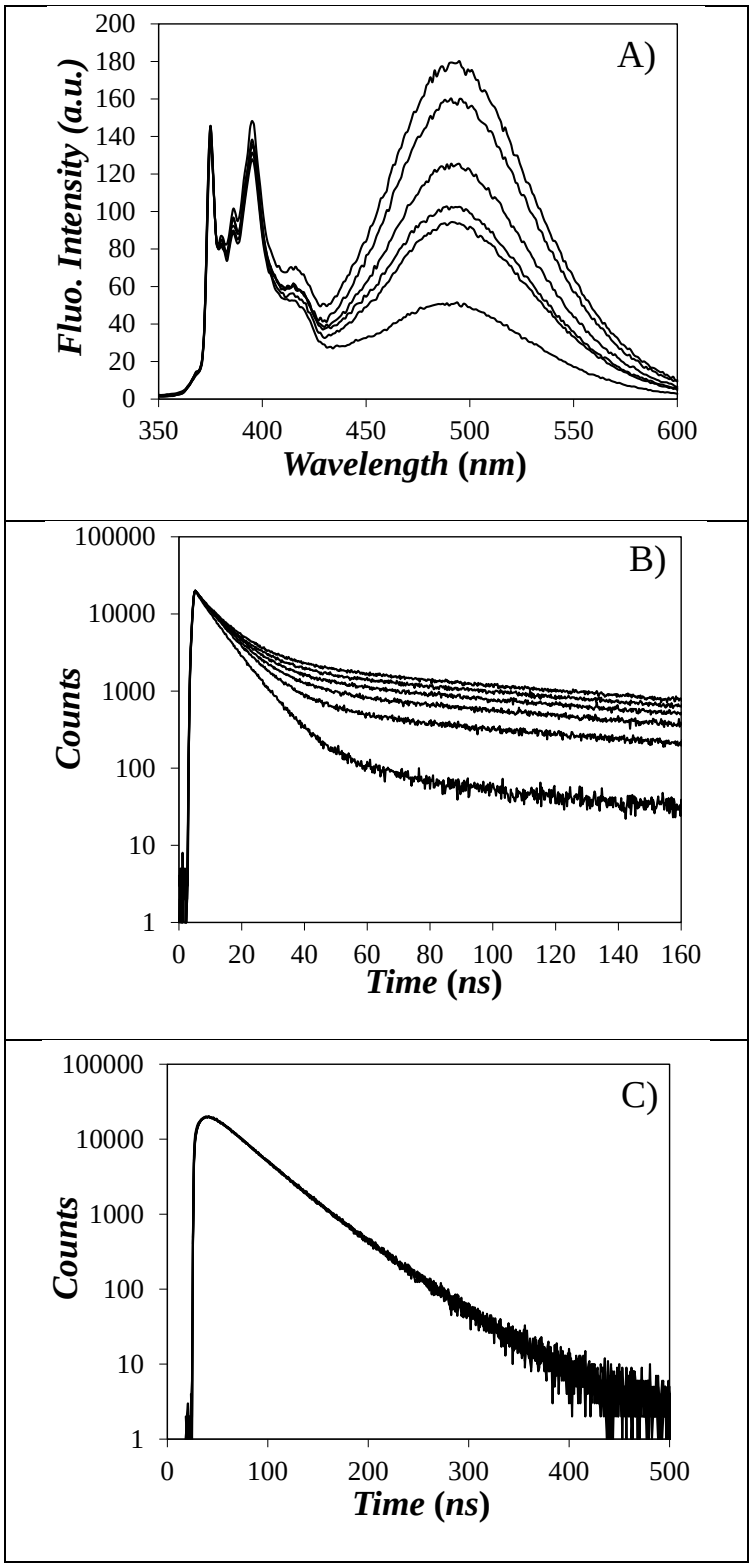

Figure 2. A) Fluorescence spectra of DiPyMe normalized at 375 nm. From top to bottom: 0, 2, 4, 6, 8, and 10 min irradiation; B) Fluorescence decays of the pyrene monomer of DiPyMe. From

bottom to top: 0, 2, 4, 6, 8, and 10 min irradiation; C) Overlapping excimer fluorescence decays. [SDS] = 50 mM, [NaCl] = 50 mM, [DiPyMe] = 2.4×10^{-6} M

Although comparison of the I_E/I_M ratio was complicated by the dependency of the monomer fluorescence to changes in salt concentration, the decrease in I_E/I_M was steepest and most pronounced in the absence of salt ([NaCl] = 0.0 M), followed by the SDS solution with 0.1 M NaCl, and then all the higher salt concentrations which yielded similar trends. The trends shown in Figure 3A indicate that the SDS solution with the lowest salt concentration experiences the fastest and most extensive degradation of DiPyMe. Incidentally, the 0.0 M NaCl solution of SDS also generated the smallest SDS micelles (see N_{agg} in Figure 1C). These conditions would allow more interactions between DiPyMe and the aqueous phase, a situation that would favor hydrolysis compared to the solutions with higher salt concentrations where the larger size of the SDS micelles would better shield DiPyMe from the water phase.

If DiPyMe does indeed hydrolyze in aqueous solutions of SDS, then it would produce two PyMeOH molecules. In turn, PyMeOH with its hydroxyl group and one hydrophobic pyrene moiety is significantly more water-soluble than DiPyMe with its less polar ether bond and two hydrophobic pyrenyl groups. Consequently, it is reasonable to expect that the hydrolysis of DiPyMe into PyMeOH would result in the migration of PyMeOH from the micellar core towards the more polar interface between the SDS micelles and the aqueous phase. The associated increase in polarity in the microenvironment of the pyrene monomer should result in an increase in the I_1/I_3 ratio. The values of I_1/I_3 were calculated from the steady-state fluorescence spectra and they were plotted in Figure 3B as a function of irradiation time for the different SDS solutions.

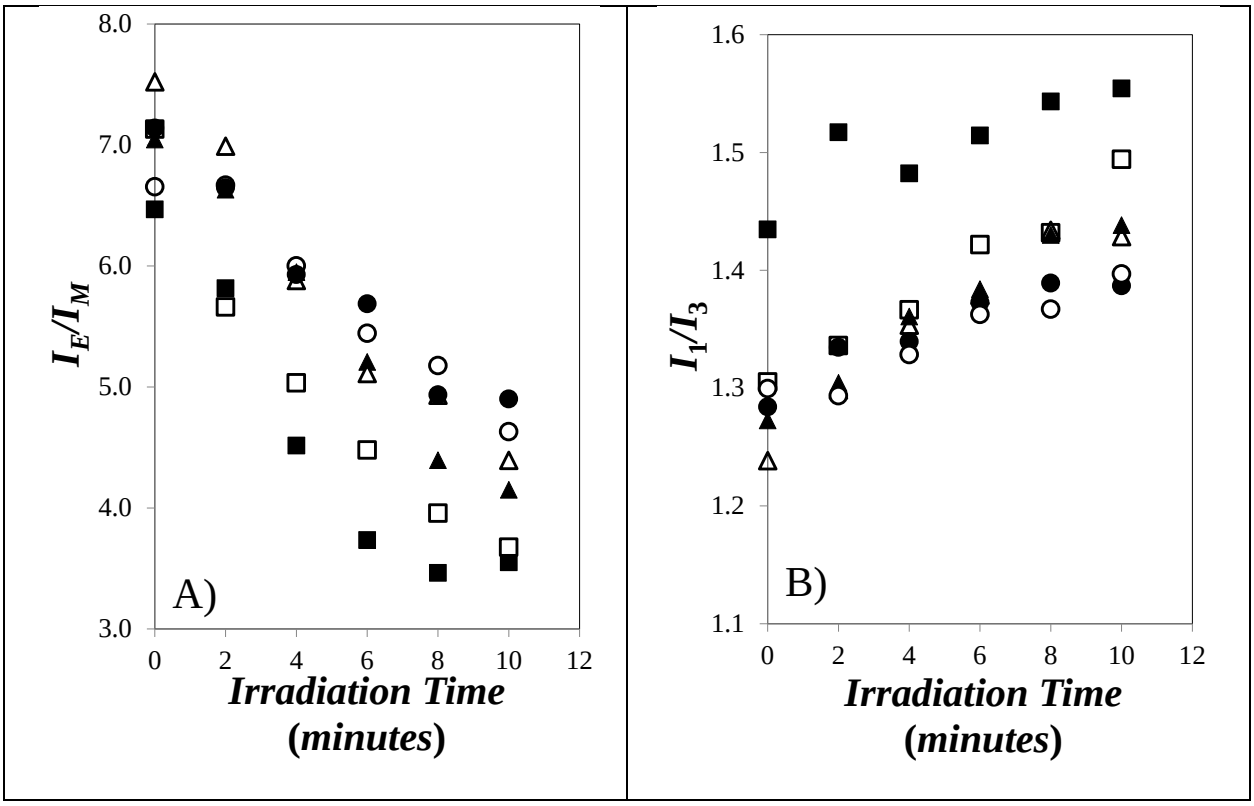

Figure 3. Plot of the ratios A) I_E/I_M and B) I_1/I_3 of DiPyMe as a function of irradiation time for 50 mM SDS aqueous solutions with NaCl concentrations of (■) 0.0 M, (□) 0.1 M, (▲) 0.2 M, (△) 0.3 M, (●) 0.4 M, and (○) 0.5 M.. [DiPyMe] = 2.4×10^{-6} M

The SDS solution without salt yielded the highest I_1/I_3 ratio, the 0.1 M NaCl solution resulted in the second highest I_1/I_3 ratio, and the SDS solutions with the higher NaCl concentrations showed overlapping trends. Again, since the zero-salt concentration yielded the smallest SDS micelles, PyMeOH could respond better to the polar environment of the water phase and thus reported a larger I_1/I_3 ratio. As the salt concentration increased, the SDS micelles increased in size (see N_{agg} in Figure 1C), thus shielding PyMeOH from the aqueous phase and resulting in smaller I_1/I_3 ratios corresponding to the decrease in local polarity experienced by PyMeOH. All DiPyMe solutions showed an increase in I_1/I_3 with increasing irradiation time as would be expected from the hydrolysis of the ether bond of DiPyMe into two PyMeOH molecules, the hydrolysis occurring

to the greatest extent at the lowest salt concentration where the smaller SDS micelles are less able to shield DiPyMe from the aqueous solution. The proposed hydrolysis of DiPyMe is shown in Equation 4 where k_h is the hydrolysis rate constant.

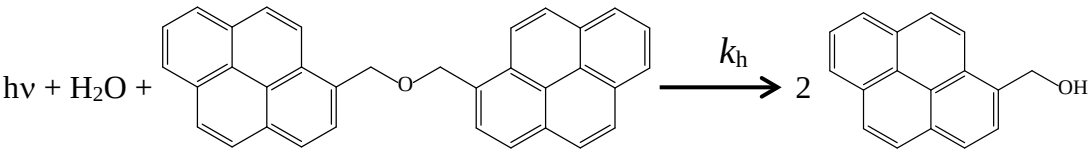

(4)

The results obtained thus far by steady-state fluorescence suggest that DiPyMe is photodegraded, probably through hydrolysis, when it is placed in the path of the excitation light for the steady-state fluorometer. To further support the plausibility of this proposal, the fluorescence decays of the monomer and excimer were acquired for the SDS aqueous solutions of DiPyMe at different irradiation times. The decays were fitted individually with sums of exponentials. Good fits were obtained with χ^2 values lower than 1.30 and residuals and autocorrelation of the residuals randomly distributed around zero. The monomer decays were first fitted using a sum of four exponentials with one lifetime fixed to 157 ns, the lifetime that was found for PyMeOH in SDS micelles. The monomer decays showed two shorter decay times of 3.2 ± 1.4 ns and 11.3 ± 1.9 ns with relatively constant and substantial contributions of 0.15 and 0.80, respectively. Since these contributions were constant, they were not expected to be due to degradation products. Rather the ~11 ns decay time in the monomer decay approximately matched the rise time in the excimer decay. The two other decay times, one ranging between 24 and 100 ns and the other set to equal 157 ns had very small contributions which increased with increasing irradiation time. These two longer decay times showing an increasing contribution were attributed to the degradation products of DiPyMe, one of them being PyMeOH. Since the shortest decay

time of 3.2 ± 1.4 ns was not observed in the excimer decay and since its contribution did not change much with irradiation time, it was attributed to an unknown quenching mechanism of the pyrene monomer without excimer formation possibly due to the hindered mobility experienced by DiPyMe inside the micelles. This left the one remaining decay time of 11.3 ± 1.9 ns that also matched the excimer risetime to be attributed to the process of diffusional excimer formation. The excimer decays could be fitted with a sum of three exponentials. The excimer decays exhibited a 12.3 ± 2.0 ns rise time and two decay times around 29 ± 4 and 48 ± 2 ns. These two last decay times are typical of a short (~30 ns) and a longer-lived (~50 ns) excimer found with pyrene-labeled molecules where excimer formation is geometrically restricted,[28,30] as would be the case for DiPyMe in SDS micelles. The ratio A_{E-}/A_{E+} of the sum of the negative pre-exponential factors over that of the positive pre-exponential factor equalled −0.85 ± 0.05, a value close to −1.0 indicating that excimer formation occurred mostly by diffusion. The decay times and their pre-exponential factors derived from the fits of the monomer and excimer fluorescence decays with a sum of exponentials can be found in Tables S1 and S2 in Supporting Information (SI).

The conclusions drawn from the analysis of the fluorescence decays with sums of exponentials led to the implementation of a program based on the Model Free Analysis (MFA). In this program, excimer formation was handled with a single coupled lifetime in the monomer and excimer decays and three uncoupled decay times were used in the monomer decays, one fixed to 3.5 ns to account for the quenching of the monomer that does not lead to excimer formation, a second floating decay time to handle some of the degradation products, and one fixed to 157 ns to describe the contribution from PyMeOH generated from the hydrolysis of DiPyMe. Two uncoupled decay times were used for the excimer decays to describe the two excimer species with lifetimes τ_E and τ_D. The two excimers were assumed to be generated with the same rate constant

<k>. The process applied to implement the MFA has been described in a number of reviews[35-37] and the equations used to fit globally the monomer and excimer decays acquired with DiPyMe in SDS aqueous solutions are provided in SI as Equations S1 and S2, respectively. As for the fits of the individual monomer and excimer decays with sums of exponentials, the MFA yielded excellent fits and all the parameters retrieved from this analysis are listed in Tables S3-S5. Fits resulting from the global MFA of the decays shown in Figures 2B and C have been provided in Figure S5 in SI.

The rate constant <k> for pyrene excimer formation of DiPyMe in SDS micelles remained constant within experimental error as a function of irradiation time in Figure 4A for a given salt concentration. The lifetimes τ_E and τ_D were found to remain constant for all salt concentrations and equal to 32 ± 2 ns and 50 ± 3 ns. The constancy of <k>, τ_E, and τ_D observed for each salt concentration was expected from the overlapping excimer decays shown in Figure 2C.

After the <k> values obtained at a given NaCl concentration were averaged over all irradiation times, the averaged <k> values were plotted as a function of NaCl concentration in Figure 4B. As for k_q in Figure 1E, <k> was found to decrease continuously with increasing salt concentration. However, whereas k_q responded to changes in both the microviscosity and volume of the interior of the SDS micelles (see Equation 3), <k> depended solely on the microviscosity since each pyrenyl unit constituting DiPyMe could not probe the interior of the SDS micelles independently of the other. Consequently, the decrease in <k> with increasing salt concentration shown in Figure 4B indicated that the microviscosity of the SDS micelles increased as the micelles increased in size, probably due to enhanced crowding of the micellar interior as N_{agg} also increased with increasing salt concentration in Figure 1C.

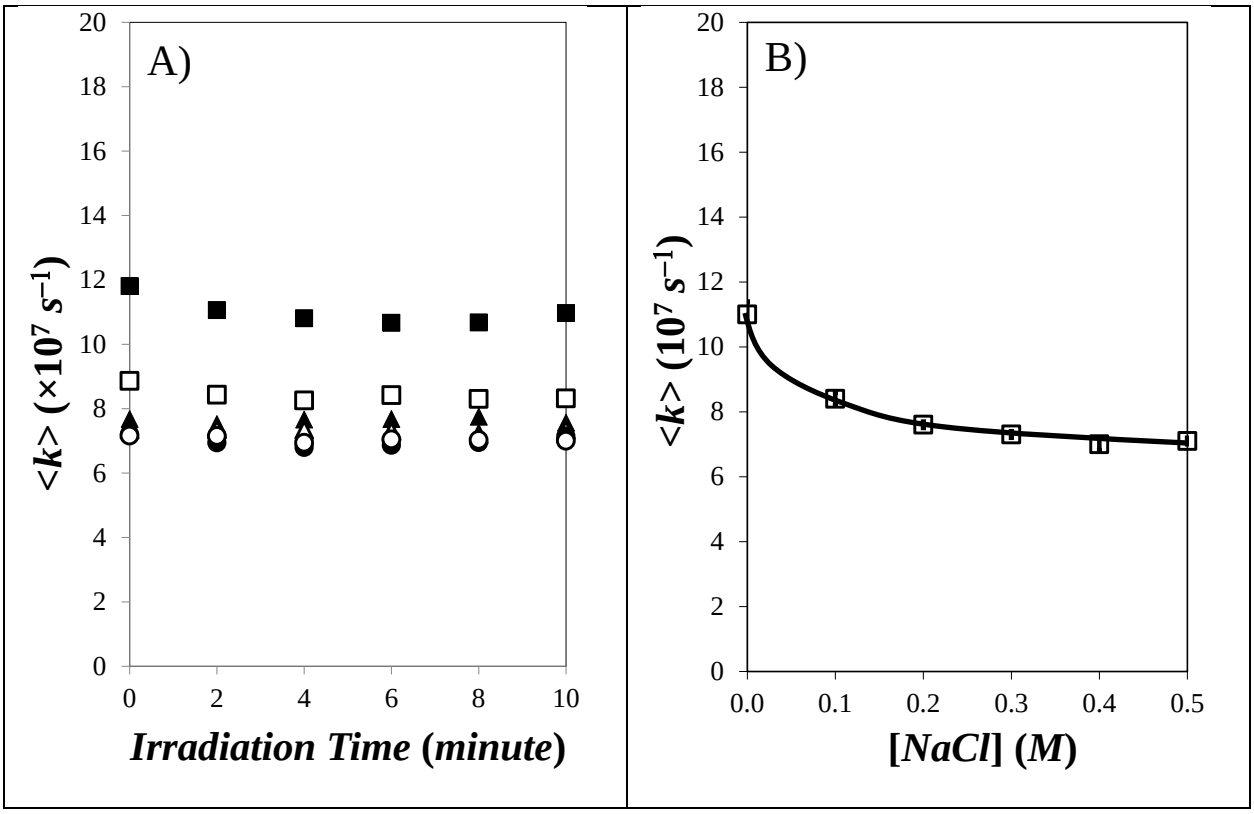

Figure 4. Plot of A) <*k*> as a function of irradiation time for samples of DiPyMe as a function of irradiation time for 50 mM SDS aqueous solutions with NaCl concentrations of (■) 0.0 M, (□) 0.1 M, (▲) 0.2 M, (△) 0.3 M, (●) 0.4 M, and (○) 0.5 M. B) Plot of averaged <*k*> values as a function of salt concentration. [DiPyMe] = 2.4×10^{-6} M.

The fluorescence fractions f_{free}, f_{diff}, f_{agg}, and f_q, which refer to, respectively, the pyrene units that cannot form excimer (i.e. isolated PyMeOH molecules in SDS micelles), form excimer by diffusion, form excimer upon direct excitation of a ground-state pyrene dimer, or are quenched without forming an excimer were also calculated from the values obtained from the MFA. Excimer formation occurred mostly by diffusion as implied from the A_{E-}/A_{E+} ratio, the MFA yielding an f_{diff} value equal to 0.66 ± 0.08, regardless of salt concentration. Nevertheless, it was also noticeable that a non-negligible fraction of the pyrene units were aggregated in the 50 mM SDS aqueous

solutions with f_{agg} = 019 ± 0.02 for DiPyMe in 50 mM SDS without salt (see Table S5). This was reflected by the low peak-to-valley ratio or P_A value of 2.0 obtained from the absorption spectrum of DiPyMe shown in Figure S1B. P_A values smaller than 3.0 usually indicate that pyrene aggregates are present in solution.[43] By comparison, a P_A value of 3.0 was obtained for the absorption spectrum of DiPyMe in THF shown in Figure S1A reflecting little pyrene aggregation as expected from the f_{agg} value of 0.05 retrieved from the MFA of the fluorescence decays of DiPyMe in THF (see Table S13). The aggregation of pyrene units in SDS micelles results from the restricted volume available to the DiPyMe molecule in the 50 mM aqueous solution.

The f_{free} values were plotted as a function of irradiation time in Figure 5A, while the other molar fractions may be found in Table S5 in SI. The fraction f_{free} was found to increase linearly with increasing irradiation time. If DiPyMe was hydrolyzing into two PyMeOH molecules according to Equation 4, then the slope of these lines would yield the rate constant of hydrolysis k_h which was plotted as a function of NaCl concentration in Figure 5B. k_h decreased with increasing salt concentration reflecting the increased difficulty to hydrolyze DiPyMe molecules as the size of the SDS micelles (see N_{agg} in Figure 1C) and the microviscosity of the micellar interior (see Figure 4B) increased with increasing salt concentration. Both effects contributed to reducing interactions between DiPyMe and the aqueous phase and led to the reduction in k_h observed in Figure 5B.

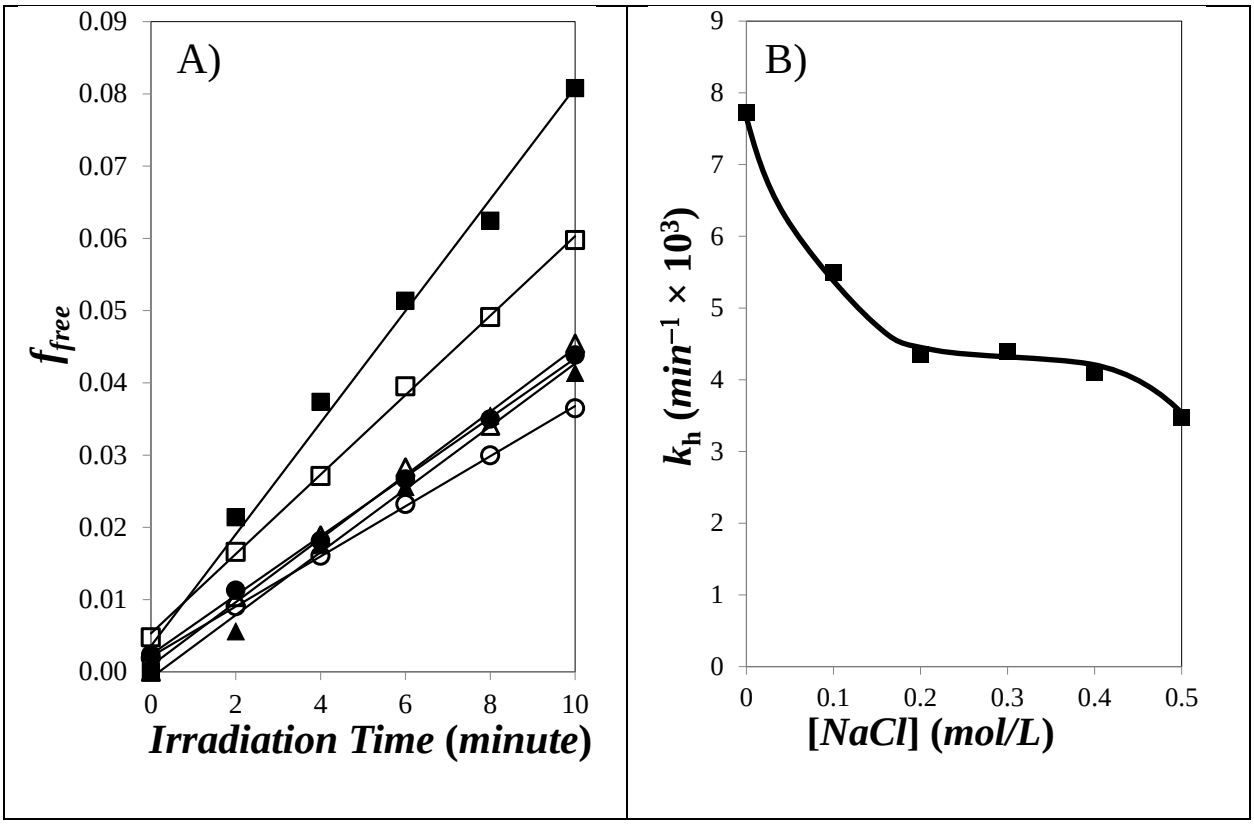

Figure 5. Plot of A) f_{free} as a function of irradiation time for samples of DiPyMe as a function of irradiation time for 50 mM SDS aqueous solutions with NaCl concentrations of (■) 0.0 M, (□) 0.1 M, (▲) 0.2 M, (△) 0.3 M, (●) 0.4 M, and (○) 0.5 M.

The decrease in the I_E/I_M ratio presented in Figure 3A as a function of irradiation time might appear to be a problem if it were used to estimate the microviscosity of the interior of SDS micelles. In practice, this problem might not be as severe as it seems. Contrary to what Figure 2A might lead the reader to believe due to the normalization of the fluorescence spectra at 375 nm, the part of the fluorescence spectrum of DiPyMe most affected by the hydrolysis is that of the pyrene monomer which is acquired within the first 10 seconds, an acquisition time over which very little degradation of DiPyMe was observed (Figure 3). Consequently, the ratio I_E/I_M obtained for a DiPyMe solution that was not irradiated beforehand cannot be affected much by the

hydrolysis of DiPyMe in aqueous solution. Only if the DiPyMe aqueous solution is continuously irradiated will the I_E/I_M ratio be affected substantially as illustrated in Figure 3.

While the I_E/I_M ratio of DiPyMe responds to the microviscosity of the environment, its value is not absolute because of the strong dependency of the I_1 intensity to the polarity of the environment. Since I_1 is selected to measure the I_E/I_M ratio to ensure good spectral separation between the monomer and excimer fluorescence signals, the value of the ratio also depends inevitably on the polarity of the environment. While this feature is advantageous to establish the location of DiPyMe in a heterogeneous solution such as an aqueous solution of SDS micelles, it represents a major drawback to measure quantitatively the microviscosity of micellar domains by comparing the I_E/I_M ratio of DiPyMe obtained in a microenvironment with that obtained in a solvent whose viscosity can be measured accurately. Fortunately, while the I_E/I_M ratio is a relative measure, the $<k>$ value reported in Figure 4B is absolute and can be compared with the $<k>$ value of DiPyMe in homogeneous solvents whose viscosity can be measured. To this end, the fluorescence spectra and decays of DiPyMe were acquired in mixtures of toluene and benzyl alcohol (BnOH) on the one hand and mixtures of DMSO and a 400 g/mol poly(ethylene glycol) (PEG(0.4K)) on the other hand. In the absence of water, the fluorescence spectra of DiPyMe in these organic solvents were unaffected by the irradiation time further supporting the notion that the presence of water in the aqueous SDS solutions is responsible for the hydrolysis of DiPyMe under UV irradiation. The fluorescence decays of the pyrene monomer and excimer were fitted according to the MFA with Equations S21 and S22, respectively. Excellent fits of the decays were obtained and the $<k>$ value for DiPyMe was determined and plotted as a function of solvent viscosity in Figure 6A.

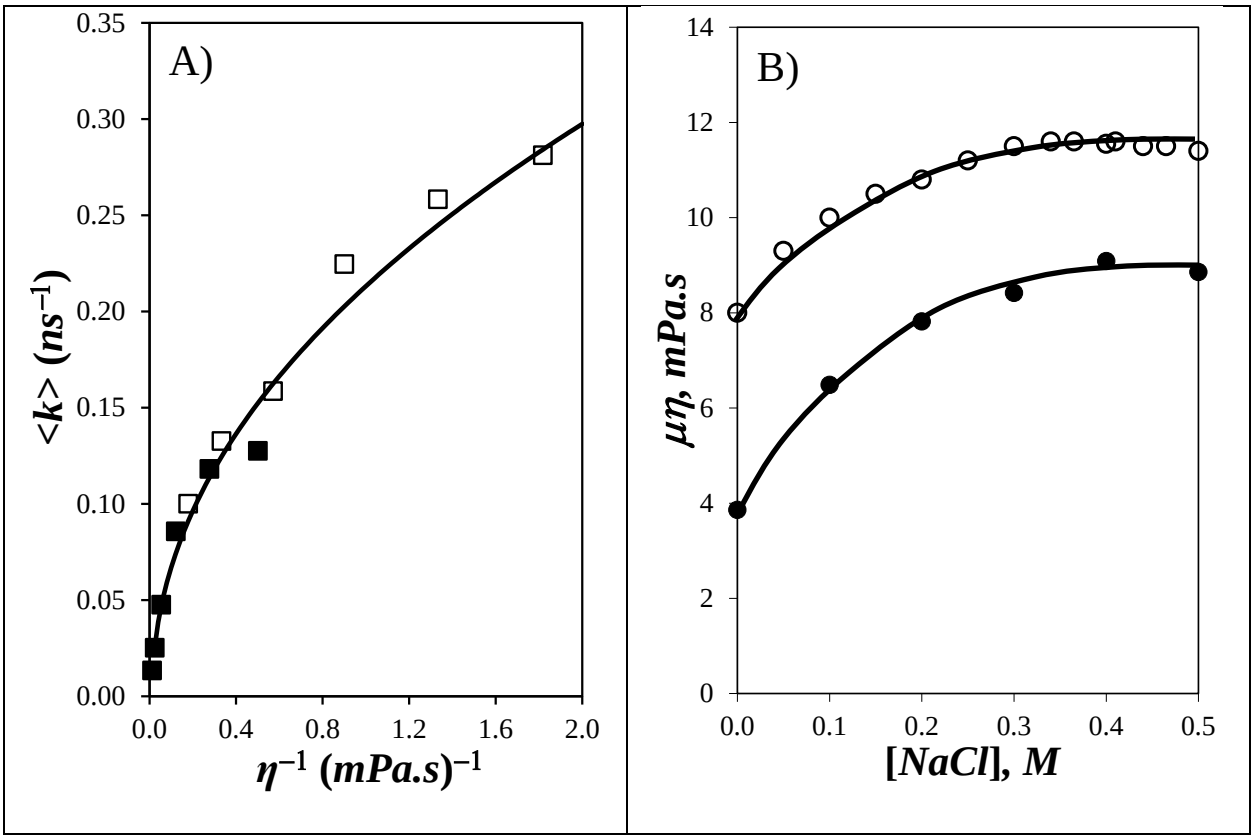

Figure 6. A) Plot of <*k*> obtained for DiPyMe in mixtures of (□) toluene and benzyl alcohol and (■) DMSO and PEG(0.4K); B) Plot of microviscosity inside SDS micelles probed by (●) DiPyMe or (○) ESR[44] as a function of salt concentration.

In the viscosity regime where η ranges between 1.6 and 5.0 mPa.s in Figure 6A, similar <*k*> values were obtained for DiPyMe in the mixtures of toluene and BnOH on the one hand and DMSO and PEG(0.4K) on the other hand. This observation confirms that <*k*> responds solely to the solvent macroscopic viscosity and not its polarity. The empirical Equation 5 was found to fit the experimental trend in Figure 6A between <*k*> expressed in ns^{-1} and η^{-1} expressed in $(mPa.s)^{-1}$ relatively well. Equation 5 was derived by noting that for η values lower than 5.6 mPa.s corresponding to <*k*> values greater than 1.0×10^{8} s^{-1}, η^{-1} scaled as $24.4\times\langle k\rangle^{2.09}$. Unfortunately this power law failed to properly describe the <*k*> vs. η^{-1} trend obtained for larger viscosities. A

plot of $\eta^{-1}/24.4\times<k>^{2.09}$ vs. $<k>$ for the high viscosity data was found to be relatively well fitted by the expression $1.0 + 1.22\times10^{-3}\times<k>^{-1.87}$. Putting the low and high viscosity regimes together resulted in Equation 5 which was applied to predict the microviscosity experienced by DiPyMe in the SDS micelles based on the $<k>$ values reported in Figure 4B. Converting the $<k>$ values obtained for DiPyMe in SDS micelles into microviscosity yielded the plot shown in Figure 6B. The microviscosity in the micelles was found to increase continuously at low salt concentration, more than doubling from 4.0 mPa.s without salt up to 8.8 ± 0.3 mPa.s at NaCl concentrations of 0.3 M and up. Above 0.3 M NaCl, the microviscosity stopped to increase. The microviscosity profile obtained with DiPyMe in Figure 6B is quite similar to that obtained by ESR using 5-doxylstearic acid methyl ester,[44] although the absolute $\mu\eta$ values are different probably due to the fact that the different probes might interact with different parts of the SDS micelles. Nevertheless the overall agreement between the two techniques that predict an increase in $\mu\eta$ with increasing salt concentration is quite remarkable.

$$\eta^{-1} = (0.001219 \times < k >^{-1.867} + 1.00) \times 24.377 \times < k >^{2.0914} \qquad (5)$$

The characterization of the micellar size (N_{agg} in Figure 1C) and the microviscosity of the micellar interior ($\mu\eta$ in Figure 6B) provided the means to compare the effect that these parameters have first on each other and second on k_q, the rate constant of pyrene excimer formation presented in Figure 1E. Figure 7A is a plot of $\mu\eta$ as a function of N_{agg}. Up to a salt concentration of 0.3 M corresponding to an N_{agg} value of 117, an increase in micellar size is accompanied by a steep increase in $\mu\eta$. This result would be expected as the more crowded micellar interior should hinder the mobility of its cargo. The more surprising result in Figure 7A is that past a salt concentration

of 0.3 M, any further increase in micellar size no longer affect $\mu\eta$. The profile of $\mu\eta$-vs-[NaCl] in Figure 7A suggests that SDS micelles undergo a transition in their morphology, most likely a change from a spherical to a cylindrical morphology occurring around 0.3 M salt concentration.[38,39,44] The existence of such a transition would explain why further increase in N_{agg} for salt concentrations larger than 0.3 M are not associated with an increase in $\mu\eta$. Elongation of a cylinder with N_{agg} increasing from 116 for a salt concentration of 0.3 M to 172 for a salt concentration of 0.5 M would provide a similar micellar interior in terms of microviscosity regardless of the cylinder length as experimentally observed in Figure 7A.

The effect that N_{agg} and $\mu\eta$ have on k_q can be seen in Figure 7B where k_q is plotted as a function of $(N_{agg}\times\mu\eta)^{-1}$. Since a larger micellar volume and microviscosity reduce the probability of encounter between two pyrene molecules hosted in a same micelle, k_q is expected to be inversely proportional to the product $(N_{agg}\times\mu\eta)$ as predicted by Equation 3. Within experimental error, two linear trends are indeed observed in Figure 7B. They are associated with two different regimes, one for salt concentrations smaller than 0.3 M where k_q takes larger values and the other for salt concentrations larger than 0.3 M where k_q takes smaller values and decreases more steeply with increasing $(N_{agg}\times\mu\eta)^{-1}$. The breakpoint between the two regimes might correspond to the salt concentration ([NaCl] = 0.3 M) where SDS micelles change from a spherical to a cylindrical morphology as has been suggested in other studies.[38,39,44]

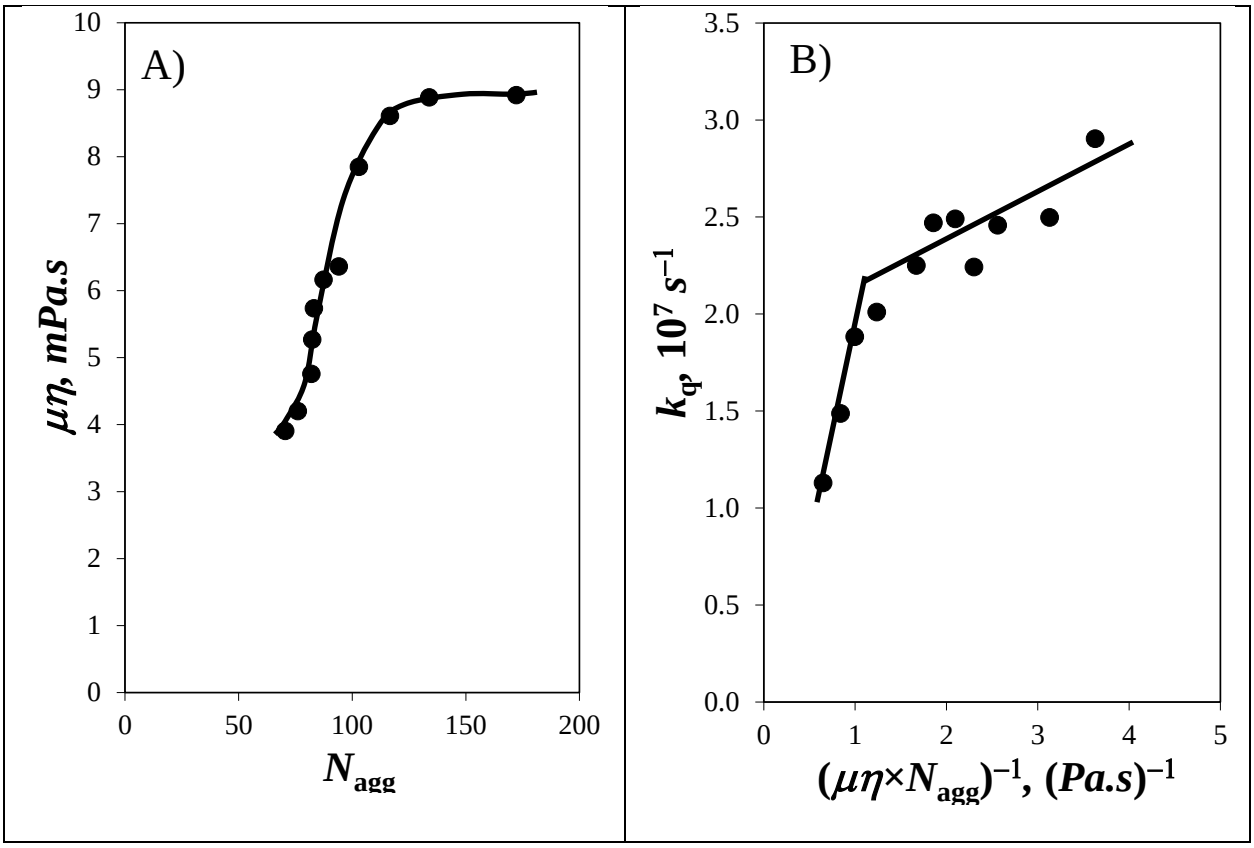

Figure 7. A) Plot of the microviscosity inside the SDS micelles probed by DiPyMe as a function of salt concentration and B) plot of k_q for pyrene excimer formation inside the SDS micelles as a function of $(\eta \times N_{agg})^{-1}$.

DISCUSSION

The determination of the microviscosity of the interior of surfactant or polymeric micelles has been an important topic of research over the past four decades. In the case of surfactant micelles, at least four general methods have been developed to determine $\mu\eta$. The first method requires the determination of k_q as done in Figure 1E for the quenching of a fluorophore by a quencher both located inside a same micelle. Applying the Einstein-Schmoluchowski expression for k_{diff} in Equation 3 which includes the viscosity of the medium yielded $\mu\eta$. This procedure resulted in values of $\mu\eta$ in SDS micelles ($\mu\eta_{SDS}$) equal to 193 mPa.s at 23 °C for pyrene excimer formation,[45]

between 15 and 36 mPa.s at RT for the quenching of pyrene by iodide anions,[46] and 3.2 mPa.s at RT for the quenching of diethylindoloindole by α–cyanonaphthalene.[47] A second procedure involves the measurement of the short subnanosecond viscosity-dependent lifetime of carboxycyanine derivatives. Comparison of the lifetime of two carboxycyanine derivatives obtained in SDS micelles and a calibration curve obtained with solvents of known viscosity yielded $\mu\eta_{SDS}$ values of 5.0 mPa.s[48] or 4.3 mPa.s[49] both at RT.

The third and most commonly employed method involves bichromophoric probes that can form excimer and whose I_E/I_M ratios in surfactant micelles is compared to the I_E/I_M ratio obtained with a calibration curve where I_E/I_M is plotted as a function of solvent viscosity. By far, the bichromophoric probe of choice has been DiPyPr for these experiments yielding $\mu\eta_{SDS}$ values of 19 mPa.s at 20 ^oC,[50] 10.1 mPa or 15.6 mPa.s at 25 ^oC,[51] 21 mPa.s at 25 ^oC,[52] 19 mPa.s at 15 ^oC,[53] and 24 mPa.s at 30 ^oC.[54] Other bichromophric molecules include diphenyl propane, 1,10-dipyrenyldecane, biphenyl ether, and dinaphthylpropane that yielded $\mu\eta_{SDS}$ values of 4 mPa.s at 20 ^oC,[50] 57.1 mPa.s and 330 mPa.s at 25 ^oC,[51] 10 mPa.s at 20 ^oC,[55] and 9 mPa.s at 22 ^oC,[56] respectively. In summary, measurements with DiPyPr result in $\mu\eta_{SDS}$ values around 21 mPa.s at RT but smaller $\mu\eta_{SDS}$ values are obtained with less hydrophobic probes such as diphenyl propane, biphenyl ether, or dinaphthylpropane suggesting that such probes are located closer to the micellar interface with water where they experienced higher mobility. Consequently, the lower $\mu\eta_{SDS}$ value of 4.0 mPa.s found for DiPyMe compared to 21 mPa.s for DiPyPr might be due to its lower hydrophobicity induced by the ether linker.

Besides the difference in polarity between DiPyMe and other bichromophoric molecules which might affect its location in the SDS micelles, another major difference was the method that was applied to determine $\mu\eta_{SDS}$ with DiPyMe in this study compared to the $\mu\eta_{SDS}$ values obtained

in earlier studies with DiPyPr. In the present study, $\mu\eta_{SDS}$ was obtained through the flexible but robust MFA of the time-resolved fluorescence decays acquired with DiPyMe. As has been shown earlier for pyrene-labeled dendimers[35,57] and a short poly(ethylene oxide) construct end-labeled with pyrene,[42] the I_E/I_M ratio of probes that form excimer efficiently such as the bipyrenyl probes used to estimate $\mu\eta_{SDS}$ is highly sensitive to the presence of residual amounts of unattached pyrene labels that are much longer-lived than the pyrenyl units constituting the bipyrenyl probe. Since the quantum yield of the pyrene monomer equals $k_{rad}\times\tau$ where the radiative rate constant (k_{rad}) does not change but the lifetime (τ) of the pyrene monomer increases about 15 fold when the pyrenyl moiety is free in solution compared to covalently linked to another pyrenyl molecule as in DiPyMe or DiPyPr, the pyrene monomer intensity (I_M) can be easily overcome by a small quantity of unattached pyrenyl label. This is a general problem with the fluorescence spectrum of these bipyrenyl probes which results typically in substantially lower I_E/I_M ratios, and thus overestimated microviscosities. This artefact is fortunately eliminated when applying the MFA to the decay fitting as was done herein as this analysis isolates the contribution of the pyrenyl moieties that form excimer by diffusion from that of the unattached pyrenyl labels.[35-37,42]

One last technique used to determine $\mu\eta_{SDS}$ has been electron spin resonance with 5-doxylstearic acid methyl ester (5-DSE). Analysis of the line width of the ESR signal yielded the rotational time of the ESR probe which in turn provided the $\mu\eta_{SDS}$ values which were plotted in Figure 6B.[44] As usual, an absolute match is difficult to obtain between different probes such as 5-DSE and DiPyMe, but the overall trend as a function of salt concentration between the two probes shows a remarkably good agreement, with $\mu\eta_{SDS}$ increasing with increasing salt concentration up to a salt concentration of 0.3 M and remaining constant at salt concentration larger than 0.3 M.

The 0.3 M NaCl concentration has also been attributed to a change in micellar morphology from spherical to tubular micelles.[39,44]

While the presence of a free pyrenyl label affects the absolute value of the I_E/I_M ratio of a bipyrenyl molecule, the I_E/I_M ratio still represents a relative measure of the microviscosity of the local environment as long as the fluorescence signal of the pyrene monomer is not overwhelmed by free pyrene labels. The problem with DiPyMe is that the I_E/I_M ratio decreases continuously with increasing irradiation time (see Figure 3A) as DiPyMe is being hydrolyzed in aqueous solution. This effect makes it more challenging to infer microviscosity values from the I_E/I_M ratio obtained by analyzing the fluorescence spectrum of an aqueous solution of DiPyMe. Nevertheless relevant information about microviscosity can still be retrieved with DiPyMe by taking advantage of the fact that DiPyMe hydrolysis occurs relatively slowly, solely upon irradiation of the solution, and affects the pyrene monomer fluorescence most. To achieve this goal, the two following precautions should be strictly adhered to. First, the DiPyMe solution cannot be irradiated before starting the acquisition of the fluorescence spectrum. Since DiPyMe hydrolysis affects mostly the fluorescence signal of the pyrene monomer that is acquired in the first 10 s of irradiation, I_M will change little during this irradiation time as long as the solution was not irradiated beforehand. This first condition implies that the settings for the acquisition of the fluorescence spectrum of a DiPyMe aqueous solution which includes adjustment of the slit width of the excitation and emission monochromators to obtain sufficient fluorescence signal must have been determined previously. Since several attempts are often necessary to find satisfactory settings to acquire a fluorescence spectrum, this leads to the second condition which requires that a DiPyMe aqueous solution that was irradiated to acquire its fluorescence spectrum be discarded after completing the spectrum acquisition. Using a fresh DiPyMe aqueous solution for each fluorescence spectrum ensures that

little DiPyMe has been hydrolyzed and that the I_E/I_M ratio retrieved from the analysis of the fluorescence spectra will be little affected by DiPyMe hydrolysis.

CONCLUSIONS

This study has used the rate constant of pyrene excimer formation of DiPyMe to determine the microviscosity of SDS micelles. The parameters describing the properties of SDS micelles such as CMC, N_{agg}, k_q, or $\mu\eta_{SDS}$ were all obtained using the fluorescence of molecular pyrene or DiPyMe. After considering differences between the probes used in other studies and DiPyMe or pyrene, all trends obtained for these parameters as a function of NaCl concentration were found to be in very good agreement with those reported in earlier studies. Considering that DiPyMe was found to hydrolyze over time resulting in a drift in the fluorescence data, the mere ability to retrieve quantitative information about the process of pyrene excimer formation for DiPyMe in SDS micelles is certainly a tribute to the robustness of the MFA that is capable of distinguishing between the photophysical processes that do or do not lead to pyrene excimer formation.

Thanks to the MFA of the DiPyMe decays, the rate constant k_h of hydrolysis of DiPyMe in aqueous solutions of SDS micelles could be determined quantitatively and was found to decrease with increasing salt concentration. This result was consistent with the overall properties of the SDS micelles whose hydrophobic interior and microviscosity were found to become larger with increasing salt concentration, both effects contributing to a reduction in the probability of DiPyMe to come in contact with water and hydrolyze. Certainly, the most important aspect of this study is that it has successfully expanded the realm of applicability of the MFA further from pyrene-labeled macromolecules to characterize the process of pyrene excimer formation in bichromophoric molecules, an area of research that so far could only be handled by the DMD model and its

variants,[28] under the toughest possible experimental conditions, those of a fluorescent probe degrading over time.

ACKNOWLEDGEMENTS

The authors thank NSERC for financial support.

SUPPORTING INFORMATION

Detailed description of the procedure used to determine the CMC and MFA of the fluorescence decays. Tables of parameters retrieved from the MFA of the fluorescence decays.

REFERENCES

1. Intramolecular Excimer Fluorescence: A New Probe of Phase Transitions in Synthetic Phospholipid Membranes. *Photochem. Photobiol.* **1980**, *31*, 539-545.
2. Zachariasse, K.; Kühnle, W. Intramolecular Excimers with α,ω–Diarylalkanes. *Z. Phys. Chem. Neue Fol.* **1976**, *101*, 267-276.
3. Yamamoto, M.; Goshiki, K.; Kanaya, T.; Nishijima, Y. Intramolecular Excimer of Di(1-Pyrenylmethyleneoxycarbonyl) Alkanes. *Chem. Phys. Lett.* **1978**, *56*, 333-335.
4. Kanaya, T.; Goshiki, K.; Yamamoto, M.; Nishijima, Y. Intramolecular End-toEnd Excimer Formation of Bis(1-pyrenylmethoxy)carbonyl)alkanes. A Study of End-to-End Collisional Frequency on a Chain Molecule. *J. Am. Chem. Soc.* **1982**, *104*, 3580-3587.
5. Snare, M. J.; Thistlethwaite, P. J.; Ghiggino, K. P. Kinetics Studies of Intramolecular Excimer Formation in Dipyrenylalkanes. *J. Am. Chem. Soc.* **1983**, *105*, 3328-3332.

6. Reynders, P.; Kühnle, W.; Zachariasse, K. A. Ground-state Dimers in Excimer-Forming Bichromophoric Molecules. 1. Bis(pyrenylcarboxy)alkanes. *J. Am. Chem. Soc.* **1990**, *112*, 3929-3939.

7. Eaton, D. F.; Smart, B. E. Are Fluorocarbon Chains "Stiffer" than Hydrocarbon Chains? Dynamics of End-to-End Cyclization in a C8F16 Segment Monitored by Fluorescence. *J. Am. Chem. Soc.* **1990**, *112*, 2821-2823.

8. Zimerman, O. E.; Weiss, R. G. Static and Dynamic Fluorescence from α,ω–Di(1-pyrenyl)alkanes in Polyethylene Films. Control of Probe Conformations and Information about Microstructure of the Media. *J. Phys. Chem. A* **1998**, *102*, 5364-5374.

9. Zachariasse, K. A.; Maçanita, A. L.; Kühnle, W. Chain Length Dependence of Intramolecular Excimer Formation with 1,*n*-Bis(1-pyrenylcarboxy)alkanes for *n*=1-16, 22, and 32. *J. Phys. Chem.* **1999**, *103*, 9356-9365.

10. Pandey, S.; Kane, M. A.; Baker, G. A.; Bright, F. V.; Fürstner, A.; Seidel, G.; Leitner, W. The Photophysics of 6-(1-Pyrenyl)hexyl-11(1-pyrenyl)undecanoate Dissolved in Organic Liquids and Supercritical Carbon Dioxide: Impact on Olefin Methathesis. *J. Phys. Chem. B* **2002**, *106*, 1820-1832.

11. Zachariass, K. A.; Vaz, W. L. C. ; Sotomayor, C. ; Kühnle, W. Investigation of Human Erythrocyte Ghost Membranes with Intramolecular Excimer Probes. *Biochim. Biophys. Acta* **1982**, *688*, 323-332.

12. Winnik, F. M.; Winnik, M. A.; Ringsdorf, H.; Venzmer, J. Bis(1-pyrenylmethyl) Ether as an Excimer-Forming Probe of Hydrophobically Modified Poly(*N*-isopropylacrylamides) in Water. *J. Phys. Chem.* **1991**, *95*, 2583-2587.

13. Winnik, F. M.; Ringsdorf, H.; Venzmer, J. Interactions of Surfactants with Hydrophobically Modified Poly(*N*-isopropylacrylamides). 1. Fluorescence Probe Studies. *Langmuir* **1991**, *7*, 905-911.

14. Sadovskii, N.; Shirov, P.; Kuzmin, M.; Lemmetyinen, H.; Ikonen, M. Fluorescence of Pyrene Intramolecular Excimers in Langmuir-Blodget Films. *Thin Solid Films* **1991**, *204*, 441-449.

15. Yekta, A.; Duhamel, J.; Adiwidjaja, H.; Brochard, P.; Winnik, M. A. Association Structure of Telechelic Associative Thickeners in Water. *Langmuir* **1993**, *9*, 881-3.

16. Nivaggioli, T.; Tsao, B.; Alexandridis, P.; Hatton, T. A. Microviscosity in Pluronic and Tetronic Poly(ethylene oxide)-Poly(propylene oxide) Block Copolymer Micelles. *Langmuir* **1995**, *11*, 119-126.

17. Hrdlovič, P.; Lukáč, I. Monosubstituted Derivatives of Pyrene. Comparison of their Spectral Behaviour in Solution and in Polymer Matrices. *J. Photochem. Photobiol. A*: *Chem.* **2000**, *133*, 73-82.

18. Claracq, J. ; Santos, S. F. C. R. ; Duhamel, J.; Dumousseaux, C. ; Corpart, J.-M. Probing the Viscous Interior of Styrene/Maleic Anhydride Copolymer Aggregates in Water by Fluorescence Spectroscopy. *Langmuir* **2002**, *18*, 3829-3835.

19. Danko, M.; Hrdlovič, P.; Borsig, E. Monitoring of Swelling of Interpenetrating Polymer Network of Polyethylene/poly(styrene-*co*-butylmethacrylate) (PE/P(S-*co*-BMA)) in Toluene and Cyclohexane Using Fluorescence Spectroscopy. *Polymer* **2003**, *44*, 389-396.

20. Dayananda, K.; Kim, M. S.; Kim, B. S.; Lee, D. S. Synthesis and Characterization of MPEG-*b*-PDPA Amphiphilic Block Copolymer via Atom Transfer Radical Polymerization and Its pH-Dependent Micellar Behavior. *Macromol. Res.* **2007**, *15*, 385-391.

21. Zachariasse, K. A.; Kühmle, W.; Weller, A. Intramolecular Excimer Fluorescence as a Probe of Fluidity Changes and Phase Transitions in Phosphatidylcholine Bilayers. *Chem. Phys. Lett.* **1980**, *73*, 6-11.
22. Dangreau, H.; Joniau, M.; De Cuyper, M.; Hanssens, I. An Intramolecular Excimer Forming Probe Used to Study the Interaction of a-Lactalbumin with Model Membranes. *Biochemistry* **1982**, *21*, 3594-3598.
23. Almeida, L. M.; Vaz, W. L. C.; Zachariasse, K. A. ; Madeira, V. M. C. Fluidity of Sarcoplasmic Reticulum Membranes Investigated with Dipyrenylpropane, an Intramolecular Excimer Probe. *Biochemistry* **1982**, *21*, 5972-5977.
24. Zachariasse, K. A.; Duveneck, G.; Busse, R. Intramolecular Excimer Formation with 1,3-Di(1-pyrenyl)propane. Decay Parameters and Influence of Viscosity. *J. Am. Chem. Soc.* **1984**, *106*, 1045-1051.
25. Kano, K.; Ishibashi, T.; Ogawa, T. Freeze-Thaw Effect on Solubilization of a Hydrophobic Fluorescent Probe in Surfactant Micelles. *J. Phys. Chem.* **1983**, *87*, 3010-3012.
26. Kano, K.; Ueno, Y.; Hashimoto, S. Fluorescence Studies on the Characterization and Solubilizing Abilities of Sodium Dodecyl Sulfate, Hexadecyltrimethylammonium Chloride, and Triton X-100 Micelles. *J. Phys. Chem.* **1985**, *89*, 3161-3166.
27. Wang, F. W.; Lowry, R. E.; Cavanagh, R. R. Picosecond Excimer Fluorescence Spectroscopy: Applications to Local Motions of Polymers and Polymerization Monitoring. *Polymer* **1985**, *26*, 1657-1661.
28. Zachariasse, K. A.; Busse, R.; Duveneck, G. ; Kühnle, W. Intramolecular Monomer and Excimer Fluorescence with Dipyrenylpropanes : Double-Exponential *Versus* Triple-Exponential Decays. *J. Photochem.* **1985**, *28*, 237-253.

29. Zachariasse, K. A.; Duveneck, G. Linear Free Energy Relationships for Excimer. *J. Am. Chem. Soc.* **1987**, *109*, 3790-3792.
30. Zachariasse, K. A.; Striker, G. Three and Only Three Excited-State Species (One Monomer and Two Excimers) in 1,3-Di(1-pyrenyl)propane. *Chem. Phys. Lett.* **1988**, *145*, 251-254.
31. Kalyanasundaram, K.; Thomas, J. K. Environmental Effects on Vibronic Band Intensities in Pyrene Monomer Fluorescence and Their Application in Studies of Micellar Systems. *J. Am. Chem. Soc.* **1977**, *99*, 2039-2044.
32. Dong, D. C.; Winnik, M. A. The Py Scale of Solvent Polarities. Solvent Effects on the Virbonic Fine Structure of Pyrene Fluorescence and Empirical Correlations with ET and Y Values. *Photochem. Photobiol.* **1982**, *35*, 17-21.
33. Dong, D. C.; Winnik, M. A. The Py Scale of Solvent Polarities. *Can. J. Chem.* **1984**, *62*, 2560-2565.
34. Lianos, P.; Lux, B.; Gerard, D. Photophysical Properties of Pyrene and its Derivatives of Biophysical Importance. *J. Chim. Phys.* **1980**, *77*, 907-912.
35. Duhamel, J. Internal Dynamics of Dendritic Molecules Probed by Pyrene Excimer Formation. *Polymers* **2012**, *4*, 211-239.
36. Duhamel, J. New Insights in the Study of Pyrene Excimer Fluorescence to Characterize Macromolecules and their Supramolecular Assemblies in Solution. *Langmuir* **2012**, *28*, 6527-6538.
37. Duhamel, J. Global Analysis of Fluorescence Decays to Probe the Internal Dynamics of Fluorescently Labeled Macromolecules. *Langmuir* **2014**, *30*, 2307-2324.
38. Mysels, K. J.; Princen, L. H. Light Scattering by Some Lauryl Sulfate Solutions. *J. Phys. Chem.* **1959**, *63*, 1696-1700.

39. Almgren, M.; Gimel, J. C.; Wang, K.; Karlsson, G.; Edwards, K.; Brown, W.; Mortensen, K. SDS Micelles at High Ionic Strength. A Light Scattering, Neutron Scattering, Fluorescence Quenching, and CryoTEM Investigation. *J. Colloid Interface Sci.* **1998**, *202*, 222-231.
40. Williams, R. J.; Phillips, J. N.; Mysels, K. J. The Critical Micelle Concentration of Sodium Lauryl Sulphate at 25 ^{o}C. *Trans. Faraday Soc.* **1955**, *51*, 728-737.
41. Almgren, M.; Lofroth, J.-E. Determination of Micelle Aggregation Numbers and Micelle Fluidities from Time-Resolved Fluorescence Quenching Studies. *J. Colloid Interface Sci.* **1981**, *81*, 486-499.
42. Chen, S.; Duhamel, J.; Bahun, G.; Adronov, A. Effect of Fluorescent Impurities in the Study of Pyrene-Labeled Macromolecules by Fluorescence. *J. Phys. Chem. B* **2011**, *115*, 9921-9929.
43. Winnik, F. M. Photophysics of Preassociated Pyrenes in Aqueous Polymer Solutions and in Other Organized Media. *Chem. Rev.* **1993**, *93*, 587-614.
44. Ranganathan, R.; Peric, M.; Medina, R.; Garcia, U.; Bales, B.; Almgren, M. Size, Hydration, and Shape of SDS/Heptane Micelles Investigated by Time-Resolved Fluorescence Quenching and Electron Spin Resonance. *Langmuir* **2001**, *17*, 6765-6770.
45. Pownall, H. J.; Smith, L. C. Viscosity of the Hydrocarbon Region of Micelles. Measurements by Excimer Fluorescence. *J. Am. Chem. Soc.* **1973**, *95*, 3136-3140.
46. Grätzel, M; Thomas, J. K. On the Dynamics of Pyrene Fluorescence Quenching in Aqueous Ionic Micellar Systems. Factors Affecting the Permeability of Micelles. *J. Am. Chem. Soc.* **1973**, *95*, 6885-6889.
47. Van der Auweraer, M.; Dederen, C.; Palmans-Windels, C.; De Schryver, F. C. Fluorescence Quenching by Neutral Molecules in Sodium Dodecyl Sulfate Micelles. *J. Am. Chem. Soc.* **1982**, *104*, 1800-1804.

48. Mialocq, J. C. Picosecond Study of Pinacyanol Photophysics. *Chem. Phys.* **1982**, *73*, 107-115.

49. Grieser, F.; Lay, M.; Thistlethwaite, P. J. Excited-State Torsional Relaxation in 1,1'-Dihexyl-3,3,3',3'-tetramethylindocarbocyanine Iodide: Application to the Probing of Micelle Structure. *J. Phys. Chem.* **1985**, *89*, 2065-2070.

50. Zachariasse, K. A. Intramolecular Excimer Formation with Diarylalkanes as a Microfluidity Probe for Sodium Dodecyl Sulphate Micelles. *Chem. Phys. Lett.* **1978**, *57*, 429-432.

51. Henderson, C. N.; Selinger, B. K.; Watkins, A. R. Solvent Effects on Intramolecular Excimer Formation of Dipyrenylalkanes. *J. Photochem.* **1981**, *16*, 215-222.

52. Lianos, P.; Lang, J.; Strazielle, C.; Zana, R. Fluorescence Probe Study of Oil-in-Water Microemulsions. 1. Effect of Pentanol and Dodecane or Toluene on some Properties of Sodium Dodecyl Sulfate Micelles. *J. Phys. Chem.* **1982**, *86*, 1019-1025.

53. Turley, W. D.; Offen, H. W. Micellar Microfluidities at High Pressures. *J. Phys. Chem.* **1985**, *89*, 2933-2937.

54. Hara, K.; Suzuki, H. High-Pressure Studies of Intrammicellar Viscosity Determined by Intramolecular Excimer Forming Probe. *J. Phys. Chem.* **1990**, *94*, 1079-1081.

55. Emert, J.; Behrens, C.; Goldenberg, M. Intramolecular Excimer \forming Probes of Aqueous Micelles. *J. Am. Chem. Soc.* **1979**, *101*, 771-772.

56. Turro, N. J.; Aikawa, M.; Yekta, A. Comparison of Intermolecular and Intramolecular Excimer Formation in Detergent Solutions. Temperature Effects and Microviscosity Measurements. *J. Am. Chem. Soc.* **1979**, *101*, 772-773.

57. Yip, J.; Duhamel, J.; Bahun, G.; Adronov, A. A Study of the Branch Ends of a Series of Pyrene-Labeled Dendrimers Based on Pyrene Excimer Formation. *J. Phys. Chem. B* **2010**, *114*, 10254-10265.

Table of Contents